A Report from the University of Vermont Transportation Research Center

Scour Damage to Vermont Bridges and Scour Monitoring

TRC Report 15-002

June 2015

Anderson, Dewoolkar, Rizzo, Huston, Frolik

UVM TRC Report #15-002

Scour Damage to Vermont Bridges and Scour Monitoring

UVM Transportation Research Center Report 15-002

June 10, 2015

Prepared by:

Ian Anderson, Graduate Research Assistant, Civil and Environmental Engineering

Mandar M. Dewoolkar, Associate Professor of Civil and Environmental Engineering, School of Engineering

Donna M. Rizzo, Professor of Civil and Environmental Engineering, School of Engineering

Dryver R. Huston, Professor of Mechanical Engineering, School of Engineering

Jeff Frolik, Associate Professor of Electrical Engineering, School of Engineering

The University of Vermont

301 Votey Hall, 33 Colchester Ave., Burlington, VT 05405

Research Sponsors:

Vermont Agency of Transportation

UVM Transportation Research Center

Acknowledgements

This work was funded by the United States Department of Transportation through the Transportation Research Center (TRC) at the University of Vermont (UVM) along with the Vermont Agency of Transportation (VAOT). These two sources of research funding are gratefully acknowledged.

Many undergraduate engineering students have participated in various aspects of this project, particularly the sensor development. These students worked (or are currently working) on the sensor development as their independent research or capstone design projects. The authors thank and acknowledge the contributions of these students including Sebastian Downs, Caleb Fields, Joseph Hasselman, Heath Hescock, Griffin Jones, Connor Lacasse, Albin Meli, Cameron Michaud, Trevon Noiva, Brendan Stringer, Adisun Wheelock and Roy Wu. The authors also thank Mr. Michael Fortney for his contribution to some of the hardware and programming associated with the sensor. The authors are also grateful to Pam Thurber for providing data on some Vermont bridges.

Disclaimer

ABSTRACT

Scour is by far the primary cause of bridge failures in the United States. Regionally, the vulnerability of bridges to flood damage became evident from the damage seen to Vermont bridges in the 2011 Tropical Storm Irene. Successfully mitigating scour-related problems associated with bridges depends on our ability to reliably estimate scour potential, design effective scour prevention and countermeasures, design safe and economical foundation elements accounting for scour potential, and design reliable and economically feasible monitoring systems. This report presents research on two particular aspects related to bridge scour – 1) System-level analysis of damage observed at Vermont bridges from Tropical Storm Irene. Example case studies are presented including description of the bridge damage, as well as the pre-storm condition of the bridges. Statistical comparison to non-damaged bridges is included to identify significant factors that determine bridge vulnerability to storm damage; and 2) Development of a low-cost scour sensor suitable for monitoring scour and redeposition continuously and communicating the readings wirelessly in real time to stake holders.

TABLE OF CONTENTS

LIST OF TABLES

LIST OF FIGURES

CHAPTER 1

INTRODUCTION

1.1. PROBLEM STATEMENT AND RESEARCH FOCUS

Scour is by far the primary cause of bridge failures in the United States (Kattell and Eriksson, 1998). The HEC-18 document (Arneson, et al., 2012) provides numerous examples of scour related bridge damage and failure. During the spring floods of 1987, 17 bridges in New York and New England were damaged or destroyed by scour. The I-90 Bridge over the Schoharie Creek near Amsterdam, NY, resulted in the loss of 10 lives and millions of dollars in bridge repair and replacement costs (FHWA, 2015). In 1985, 73 bridges were destroyed by floods in Pennsylvania, Virginia, and West Virginia. A 1973 national FHWA study of 383 bridge failures caused by catastrophic floods showed that 25 percent involved pier damage and 75 percent involved abutment damage. The 1993 flood in the upper Mississippi basin caused damage to 2,400 bridge crossings (FHWA, 2015) including 23 bridge failures. The modes of bridge failure included 14 from abutment scour, 3 from pier and abutment scour, 2 from pier scour only, 2 from lateral bank migration, 1 from debris load, and 1 from unknown scour (Arneson, et al., 2012). In recent years, flooding, coastal inundation, and scour of bridge piers and abutments have been among the leading causes of bridge failures in the United States (FHWA 2015). Recent examples in the United States include numerous bridges affected by flooding, inundation, or scour in New Orleans and along the Gulf Coast in Hurricanes Katrina and Rita in 2005 (FHWA 2015).

Regionally, the aftermath of recent flooding following Tropical Storm Irene is evident in the example photographs shown in Figure 1.1. Tropical storm Irene had unprecedented impacts on transportation infrastructure in numerous regions of the New England states and the state of New York. In Vermont alone, over 300 bridges and over 900 culverts were damaged. Damages from scour and erosion (Figure 1.1) were extensive. Climate data show that Vermont is experiencing more extreme events, and that this trend is predicted to continue with more significant floods and major flooding (Frumhoff et al., 2007; Stager and Thill, 2010; Betts, 2011) demanding more resilient approaches to scour and erosion mitigation.

Successfully mitigating scour-related problems associated with bridges depends on our ability to reliably estimate scour potential, design effective scour prevention and countermeasures, design safe and economical foundation elements accounting for scour potential, and design reliable and economically feasible monitoring systems. This report presents research on two particular aspects related to bridge scour – 1) system-level analysis of damage observed at Vermont bridges following Tropical Storm Irene, and 2) development of a low-cost scour sensor suitable for monitoring scour and redeposition continuously and communicating the readings wirelessly in real time to stake holders.

(a) Scour behind an abutment of a bridge in Ludlow, VT (source: Burlington Free Press)

(b) Abutment scour in Dummerston, VT (Source: VAOT)

Figure 1.1: Example effects of scour and erosion from TS Irene on transportation infrastructure

1.2. BRIDGE SCOUR

Scour is the leading cause of bridge failure in the United States, with 20,904 bridges listed as scour critical nationwide (Gee, 2008). Scour can be categorized into three main processes: long-term aggradation and degradation of the river bed due to erosion and deposition of materials, general scour resulting from contraction of the flow, and local scour caused by a disturbance of the water flow at piers or abutments (Arneson et al., 2012). In addition to these three scour processes, lateral steam migration should also be considered in the bridge design process (Arneson et al., 2012). Although each of these fluvial processes likely played a role in damaging Vermont bridges during high storm events such as Tropical Storm Irene, contraction scour and local scour appear to be the most prevalent.

Scour design recommendations are outlined in HEC-18 (Arneson et al., 2012) with the scour depth calculated as the sum of the three above-mentioned scour components. The long-term vertical stream changes (i.e. degradation and aggradation) are classified between live-bed and clear-water scour. They are related to the upstream and in-structure soil particle sizes and stream energy and may take several storm events to cause significant damage (Arneson et al., 2012). When designing a new structure, estimates of the aggradation and degradation conditions are outlined in HEC-20 (Lagasse et al., 2012).

The second component, contraction scour, occurs when the flow area is constricted or reduced, resulting in increased velocities and stream energy, as occurs when stream flows pass beneath a bridge. Limitations on the ability of the stream to access the floodplain, obstructions placed in the floodplain, and debris interfering in the free flow of water can all result in flow constriction. By reducing the available flow area, the velocity, and therefore the energy, of the stream will be increased. The third scour type, local scour, is the result of flow disturbances as the water passes the bridge structure. Local scour is responsible for scour holes, present above and below abutments and piers. The size, shape and location of the scour depend on the alignment and size of the object. Local scour is a continuous process, but the magnitude and extent increases with stream energy, additional disturbances, and bed load.

To understand how scour related processes can damage bridges particularly in extreme events such as Tropical Storm Irene at a system-wide level, available data on Vermont bridges were analyzed to assess the level and characteristics of damage as the first component of this research. The second component included preliminary development of a low-cost scour sensor suitable for monitoring scour and redeposition continuously, and communicating the readings wirelessly in real time to stake holders. A number of scour sensing technologies have been developed (e.g. scour rod, float out devices, sonar) or currently under development (e.g. time domain reflectometry, smart rocks). The scour sensor discussed here is called a “smart rod”.

1.3. ORGANIZATION OF THIS REPORT

The remainder of this report comprises three additional chapters. Chapter 2 presents a system-level statistical analysis of damage observed at Vermont bridges from Tropical Storm Irene. Example case studies are presented including description of the bridge damage, as well as the pre-storm condition of the bridges. Statistical comparison to non-damaged bridges is included to identify significant factors that determine bridge vulnerability to storm damage. Chapter 3 documents progress made in the development of a low-cost scour sensor potentially suitable for monitoring scour and redeposition continuously, and communicating the readings wirelessly in real time to stake holders. Recommendations for future research are discussed in Chapter 4.

CHAPTER 2

SYSTEM-LEVEL ANALYSIS OF DAMAGE OBSERVED AT VERMONT BRIDGES FROM THE 2011 TROPICAL STORM IRENE

2.1. INTRODUCTION

This chapter presents a system-wide statistical analysis of Vermont bridges affected in Tropical Storm Irene in August of 2011. Example case studies include descriptions of the bridge damage, as well as the pre-storm condition of the bridges. Statistical comparison to non-damaged bridges is included to identify significant factors that determine bridge vulnerability to storm damage.

2.2. TROPICAL STORM IRENE

On August 28, 2011 the state of Vermont was severely hit by Tropical Storm Irene. The storm caused major damage throughout the state, with 223 of Vermont's 251 towns impacted. Irene entered Vermont with sustained winds of 50 mph and deposited 100-200 mm (4-8 inches) of rain across the state. Figure 2.1 shows the 12-hr average recurrence interval (ARI) from Tropical Storm Irene, based on rainfall observations collected by the National Weather Service (NWS, 2011). Particularly heavy rainfall was located to the west of the storm track, especially on the slopes of the Green Mountains. At higher elevations the intense rain caused flash flooding, and widespread flooding throughout Central and Southern Vermont, resulting in the second worst flooding event on record, following the storm of November 1927, in which a tropical storm dropped 150 mm (6 inches) or more of rain over a three day period. Both storms were preceded by a series of higher than average rainfall events, resulting in saturated ground conditions, exacerbating flood conditions. Tropical Storm Irene had a rainfall recurrence interval for a twelve-hour storm that exceeded 500 years in some areas. It caused record streamflows in nine Vermont streams, and nine other streams had peak flows among the top four on record (USGS, 2011). The occurrence of such severe events coincides with the observation that extreme rainfall events, those ranging in the 99th percentile of intensity, are happening more frequently, especially in the past three to five decades (Melillo et al., 2014).

2.3. BRIDGE DATA COLLECTION

To aid in the prediction of scour vulnerability, characteristics associated with bridges damaged in Tropical Storm Irene were compared to those associated with non-damaged bridges. Bridge inspection data will be used for comparison. To this end, a comprehensive list of all state hydraulic bridges was created and then supplemented with the available information on bridge damage from the Tropical Storm Irene. Within Vermont, multiple record systems are maintained for the purpose of asset management, with bridges being housed on various lists due to ownership and inspection responsibility. Without a comprehensive identification system, or list, it can be difficult to determine the correct records that correspond to a given bridge. News reports and estimates of bridge damage put the number at 389 damaged bridges (Thomas et al., 2013). The authors have made every attempt to identify all bridges damaged in Tropical Storm Irene, as described below.

In studying the effects of Tropical Storm Irene on Vermont's bridge infrastructure, all available bridge records were collected to generate a comprehensive list of bridge structures prior to Tropical Storm Irene. The records include identifying the geo-referenced location and information for all waterway bridges, including all available inspection data. Within Vermont, 4,832 hydraulic bridge structures were identified from the Vermont Agency of Transportation (VAOT) Bridge Inventory System (BIS), the State Short Structure Inventory Lists, and the Regional Planning Commission's (RPCs) Vermont Online Bridge and Culvert Inventory Tool (VOBCIT). The 4,832 bridges comprise both state and town hydraulic bridges of all lengths. The BIS contains all long-structure bridges (span >20ft), both state and town owned. The data associated with each bridge contains 233 items of information, including identification and geo-referenced location, as well as the results of the VAOT bridge inspections. The State Short Structure Inventory contains the state highway small structures (span <20ft) that are not included in the NBIS inspections, yet still state-owned. The VOBCIT list is comprised of town short bridges and culverts from around the state, compiled by the various RPCs. For the purposes of this study, we compiled a comprehensive list of all *scourable* bridge structures, including traditional bridges, stone arches, and open bottom culverts, and applied the general term "bridge" to all. Closed bottom culverts were then removed from the list, as they are not prone to scour damage in the same manner as a bridge, resulting in a total of n = 4,832 scourable bridge structures.

Given this comprehensive list, a record of bridge damage resulting from Tropical Storm Irene was identified. The damage of state and town bridges was provided by the VAOT and the Vermont Department of Emergency Management (VDEM), respectively. VDEM collected town bridge damage for the purpose of applying for FEMA repair funding. Bridge damage records were linked to the comprehensive bridge list to identify the location and number of affected bridges, and in some cases, a geospatial analysis was performed when database errors prevented the proper linking for identification of the bridge details. The cross referencing resulted in 153 bridges from the comprehensive bridge list being identified as damaged during Tropical Storm Irene. In a second pass at identifying and quantifying bridge damage, a thorough study of all available photographs (via the VAOT online bridge inspection photograph collection labeled with damage as well as all photos taken during the post-Irene timeframe) identified an additional 174 Irene-damaged bridges. This resulted in a total of 326 Vermont bridges identified as damaged during Tropical Storm Irene, with damage ranging from minor streambank erosion to entire bridge collapse. Of the 326 damaged bridges identified through this analysis, 27 were town short structures, and do not contain inspection information, reducing the number of damaged bridges with inspection records to 299. The locations of these 299 damaged bridges, along with the locations of the 4,506 non-damaged hydraulic bridge structures from the comprehensive list are shown in Figure 2.1. The rainfall recurrence intervals from Tropical Storm Irene are also shown in Figure 2.1.

2.4. CHARACTERIZING BRIDGE DAMAGE

Bridge damage from Tropical Storm Irene was categorized based on photographs or recorded observations and reports when photographs could not be found. Bridge damage was categorized into one of four types - scour, channel flanking, superstructure damage, and debris blockage, with the most destructive type being used to label the damage. The majority (61%) of bridge damage was the result of scour, defined as the removal of streambed and channel banks from within the bridge abutments. Channel flanking, the erosion of the approach embankment behind the bridge abutments and specifically not within the channel, was responsible for 27% of the damaged bridges. Debris blockage was observed at 5% of the bridges, at which no other hydraulic damage was seen. Debris accumulation was common across the range of the damaged bridges. Examples of each type of bridge damage are provided in Figure 2.2 - Figure 2.5.

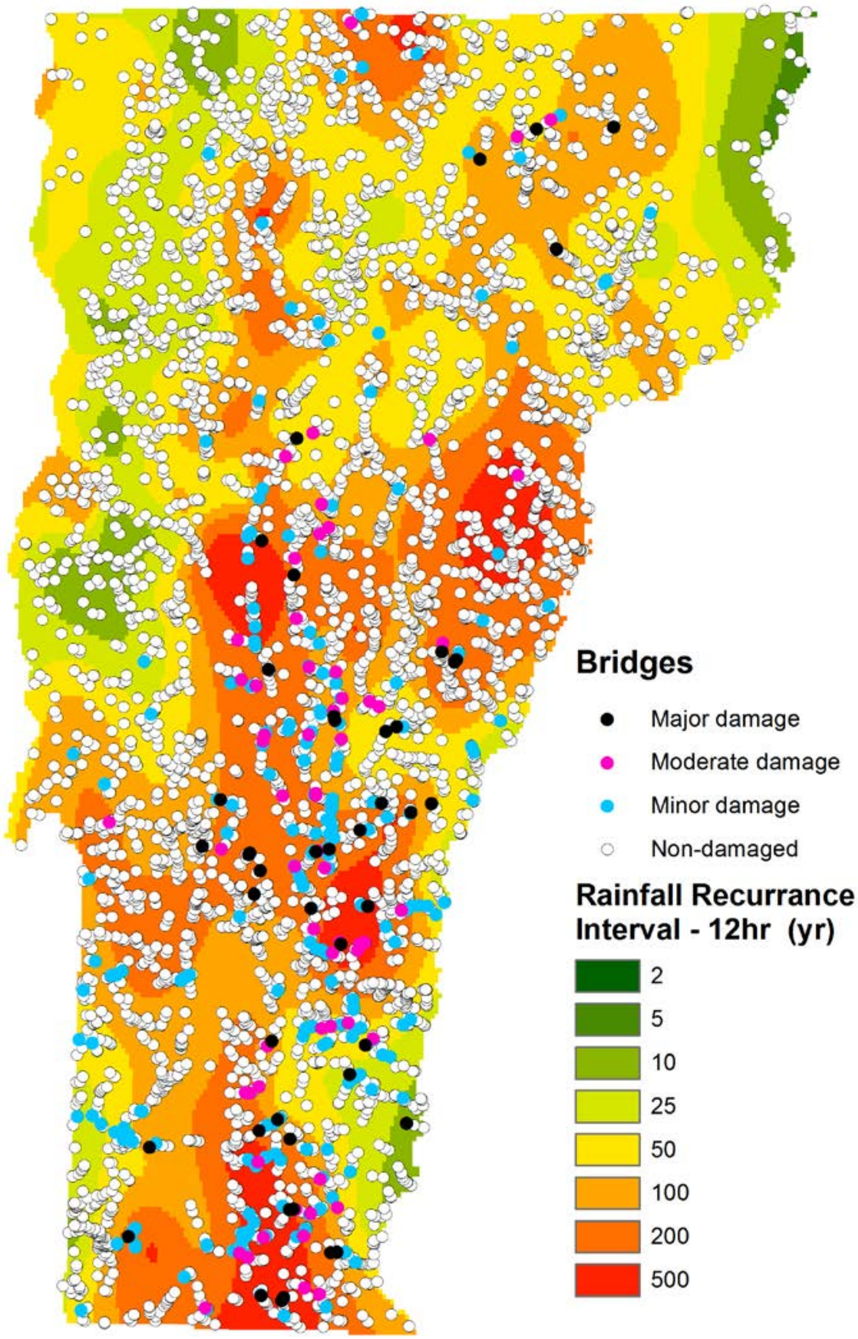

Figure 2.1: Bridge locations and rainfall from Tropical Storm Irene

(a) Clarendon US7-B96 Bridge: scour beneath the foundation, exposing several feet of wooden piles

(b) Dummerston VT30-B9 Bridge: scour beneath the concrete spread footing, with settlement resulting in the cracking of the foundation.

Figure 2.2: Examples of scour damage (VAOT, 2014)

(a) Braintree VT112A-B6 Bridge: erosion behind the wing-walled abutment, with complete loss of the bridge approach

(b) Jamaica VT30-B40 Bridge: flanking behind the abutment undermining the approach slab

Figure 2.3: Examples of channel flanking damage (VAOT, 2014)

(a) Wallingford VT140-B10 Bridge: debris buildup on a pier, reducing the flow area

(b) Wilmington VT100-B53 Bridge: obstructions at a small single span resulting in blockage and overtopping

Figure 2.4: Examples of debris damage (VAOT, 2014)

(a) Montgomery C2001-B5 Bridge: damage to the sideboards of a covered bridge

(b) Marlboro C3014-B23 Bridge: damage to the main beam of the bridge from debris impact

Figure 2.5: Examples of superstructure damage (VAOT, 2014)

The type of bridge damage was further categorized by the authors into 3 levels: major, moderate and minor (examples provided in Figures 2.6-2.8). Minor damage is damage that can be repaired using basic construction equipment and practices without requiring any engineering analysis. Examples include backfilling the approach, or adding replacement riprap. Bridge damage is categorized as moderate when the bridge has become unstable and requires engineered repairs. This would include scour beneath foundations or physical damage to bridge members.

Major damage is that which requires the rebuilding or replacement of the structure. Examples of major damage include cases where the bridge was washed away or has significant foundation settlement requiring replacement. Damage level and type were determined through observation of the pre- and post-storm inspection photos when available. When photos were not available, records from bridge inspections were used to quantify and characterize the damage. Characterizing the level and type was done without knowledge of the repair costs. Of the damaged bridges, 66% were categorized as having minor damage, 20% as having moderate damage, and 14% as having major damage.

The VDEM list of damaged bridges included cost estimates for repairing the bridge back to its pre-storm condition. A comparison of bridge damage level to the cost of repair, in U.S. dollars and dollars per deck area is shown in Figure 2.9. The horizontal line within each box plot represents the median, the edges of the box are the 25th and 75th percentiles, and the whiskers extend to the most extreme data points not considered outliers. Outliers are plotted individually, and the asterisks indicate the mean. Figure 2.9 shows that the cost of overall repair corresponds well with increasing levels of damage, and when normalized by deck area, provides a good trend among their averages. When bridge damage, represented as cost per square foot of deck area, is partitioned by damage type (Figure 2.10), it can be seen that scour damage has a much greater cost whereas the damage due to flanking is well below (less than \$200/ft^2) damage.

(a) Wardsboro VT100-B68 Bridge: flanking erosion behind the abutment, and minor scour to the footing

(b) Warren FAS188-B6 Bridge: Channel erosion and flanking behind the wingwall, with scour hole at the toe

Figure 2.6: Examples of minor damage (VAOT, 2014)

(a) Halifax C2001-B17 Bridge: loss of original riprap and backfill, resulting in the free standing abutments and scour to beneath the footing of the spread footing base

(b) Jamaica VT30-B78 Bridge: flanking behind the wingwall abutment, with scour beneath the bridge foundation, with no apparent damage to the concrete foundation, and no major settlements to the foundation

Figure 2.7: Examples of moderate damage (VAOT, 2014)

(a) Brownington C2001-B9 Bridge: fracture to the foundation, due to scour beneath the footing and settlement of substructure

(b) Moretown C3024-41 Bridge: collapse of the steel truss bridge from the apparent loss of one of the bridge foundations

Figure 2.8:Examples of major damage (VAOT, 2014)

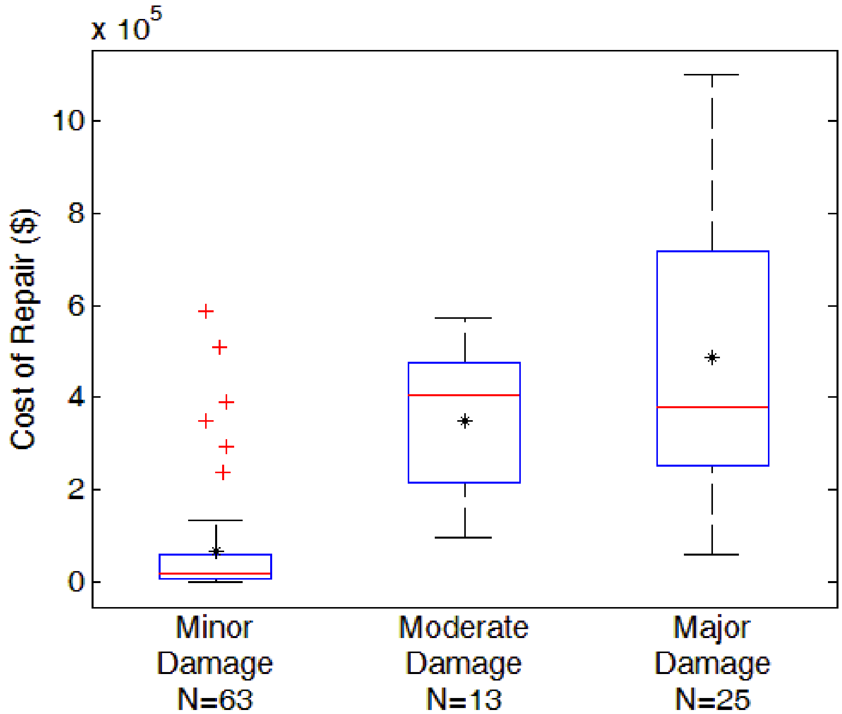

(a) Estimated cost of repair versus damage level

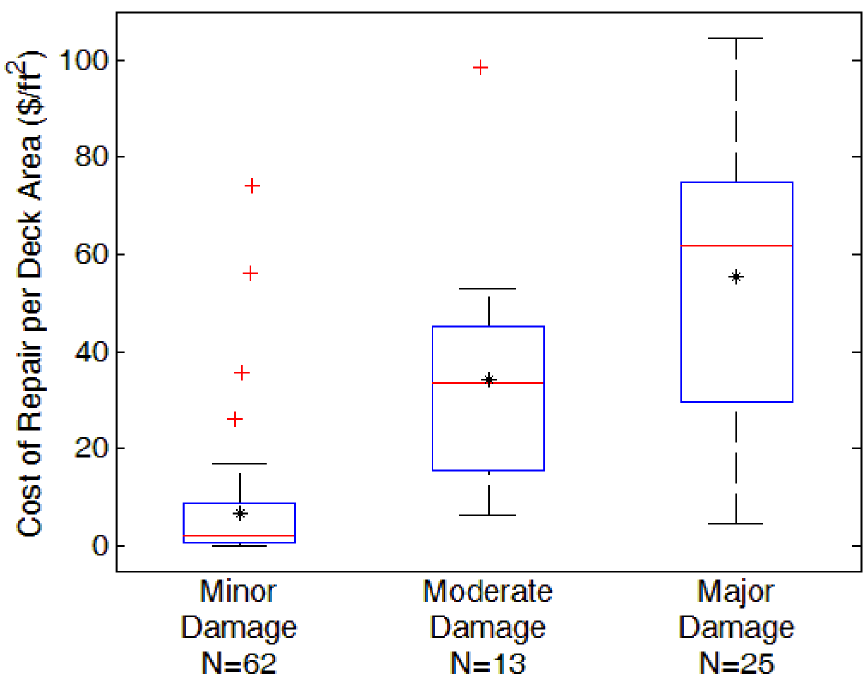

(b) Estimated cost of repair per deck area versus damage level

Figure 2.9: Estimated cost of repair, and estimated cost of repair per area for Town bridges

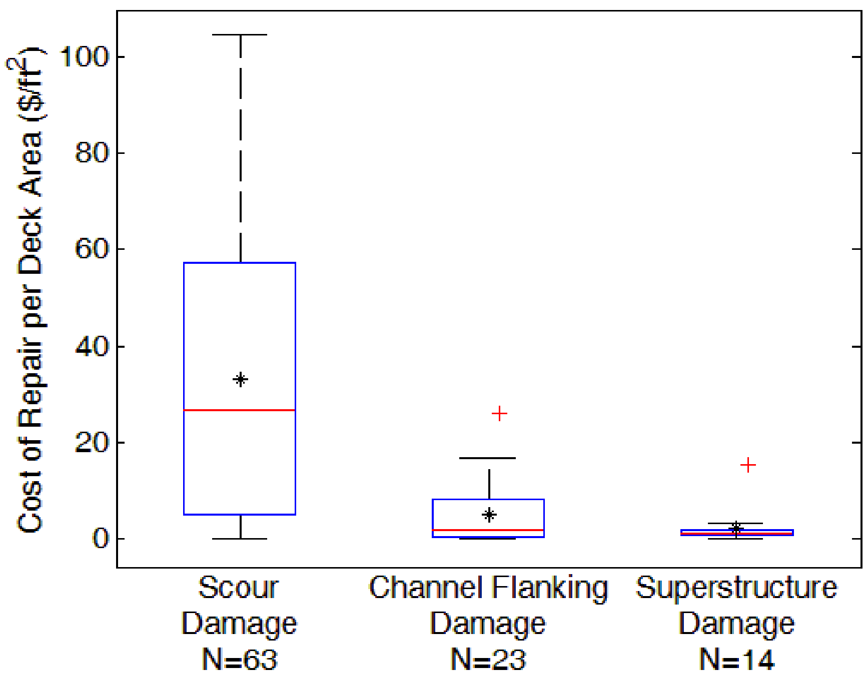

Figure 2.10: Estimated cost of repair per deck area versus type of damage

2.5. DATA COMPOSITION

The VAOT records of state and local bridges, all hydraulic long structure bridges in the BIS, as well as state and town hydraulic short structures were indexed on a statewide map using a GIS analysis. The damage information was then spatially joined to the statewide bridge records using identification information and location detail to ensure a correct match. The result of this GIS analysis includes 4,832 listings, of which 1,285 are town long bridges, 2,335 are town short bridges, 964 are state long structures, and 177 are state short structures. A subset of this comprehensive list was selected for analysis based on whether the bridge had BIS inspection records. The latter excludes town short structures. This spatial analysis results in two subsets of bridges that are used for further statistical comparison – one subset contains 299 damaged long-structure bridges, and the other contains 1,950 statewide non-damaged long-structure bridges.

2.6. RESULTS AND DISCUSSION

In total, 14 variables were tested for statistical significance between the damaged and non-damaged bridge groups using one-way ANOVA. The variable names and their resulting p-values are provided in Table 2.1. The threshold for significance was set at 0.05.

Table 2.1: One way analysis of variance

Variable	p-value
Tropical Storm Irene Parameters	
Rainfall (in)	<0.001
ARI (yr)	<0.001
Bridge Inspection Parameters	
Year Built	<0.001
Average Daily Traffic	0.0191
Structure Length (ft)	0.4319
Deck Width (ft)	0.6098
Vertical Clearance (ft)	0.0241
Deck Rating	0.0002
Superstructure Rating	<0.001
Substructure Rating	<0.001
Channel Rating	<0.001
Waterway Adequacy	<0.001
Scour Critical Rating	<0.001
Federal Sufficiency Rating	<0.001

2.6.1. Parameters Related to Tropical Storm Irene

The rainfall and average annual recurrence interval (ARI) were interpolated over the entire state, using data collected from 54 locations, and the magnitude of the impact of Tropical Storm Irene was superimposed on the bridges in Vermont (Figure 2.1).

The left-hand panels of Figures 2.11 - 2.12 show a series of histograms for the two bridge groups (i.e., non-damaged [shown in blue] and damaged [shown in red]) that plot the variable being tested on the x-axis, and the percent of the bridge population on the y-axis. Corresponding box plots for each of the two groups are plotted in the panels to the right. The horizontal line within each box represents the median, the edges of the box are the 25th and 75th percentiles, and the whiskers extend to the most extreme data points not considered outliers. Outliers are plotted individually, and the asterisks indicate the mean. Variables tested for each of the two groups are shown on the y-axis.

Figure 2.11 shows the rainfall to be significantly higher for the damaged bridge group than for the state as a whole. The ARI for damaged bridges was greater than 200 years, showing Irene was quite a significant event.

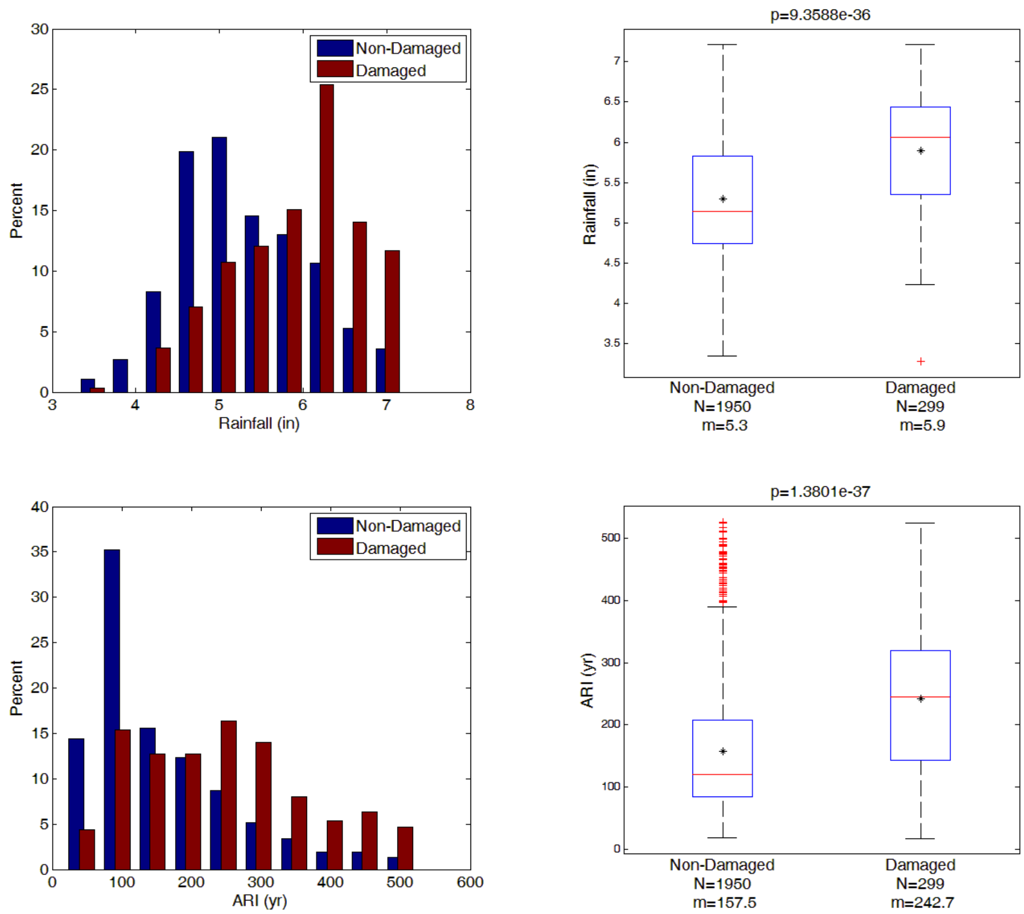

Figure 2.11: Rainfall and ARI for Tropical Storm Irene

2.6.2. Bridge Inspection Parameters

Through the creation of a comprehensive bridge inventory, the damaged bridges were identified, and their inspection records were accessed. Using the NBIS records, the bridge history, geometry, and inspection ratings are available. Results of the analysis of the bridge inspection variables can be seen in Figure 2.12.

Bridge geometry, can be summarized by the structure length, width and vertical clearance of the bridge. Length and width are not significantly different between damaged and non-damaged bridges, showing that damage was related to a factor other than the size and capacity of a bridge. The vertical clearance shows a significant difference, with damaged bridges having a lower value. The low clearance may have been related to the amount of debris observed in damage inspections, or have led to potential superstructure damage. Because of the magnitude of discharge in the flooded streams, it was hypothesized that damaged bridges might have had shorter spans, but that is not evident from the structure length alone.

Analysis of bridge inspection parameters show that bridges damaged in Tropical Storm Irene were significantly older, and had poorer inspection ratings. The ratings for damaged bridges were significantly lower for the following categories: deck, superstructure, substructure, channel, waterway adequacy, scour, and federal sufficiency rating. The pre-storm condition of the damaged bridges was lower, and there appears to be a select group of bridges that had critical ratings prior to the storm. The sufficiency rating is a collection of the prior ratings, and is used as an overall indicator. Further analysis will be needed to determine if the numerous low ratings correspond to a set of deficient bridges. The scour rating, though significantly lower for damaged bridges, still has over 50% of damaged bridges rated as non-scour critical. These results indicate that a low rating may show vulnerability to scour, however, a high rating does not show immunity particularly in an extreme event such as Tropical Storm Irene.

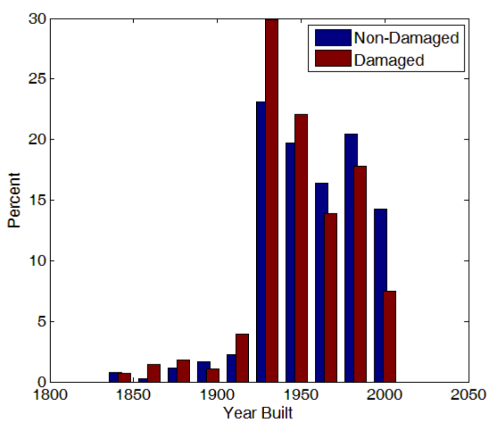

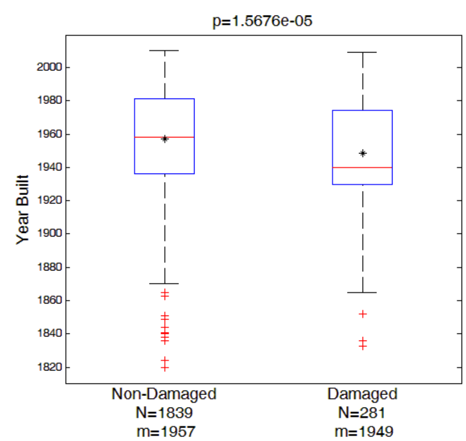

(a) Comparison with respect to the age of the bridge

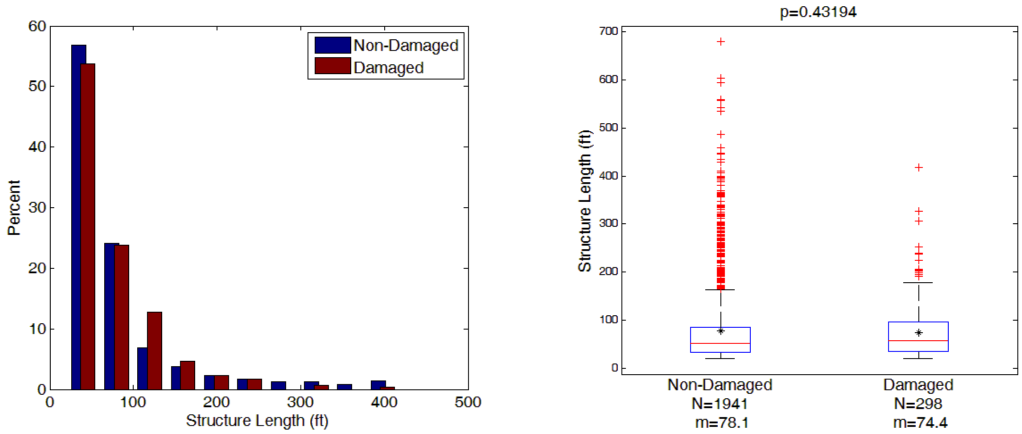

(b) Comparison with respect to the length of the structure

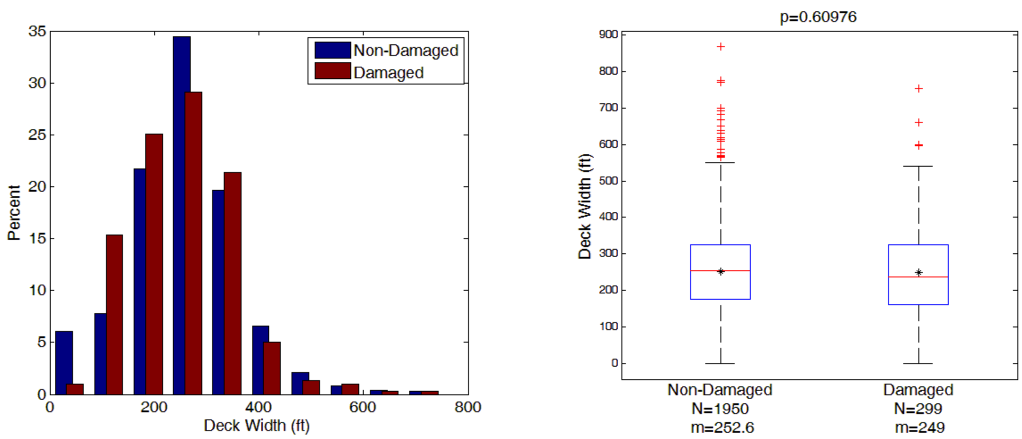

(c) Comparison with respect to the deck width

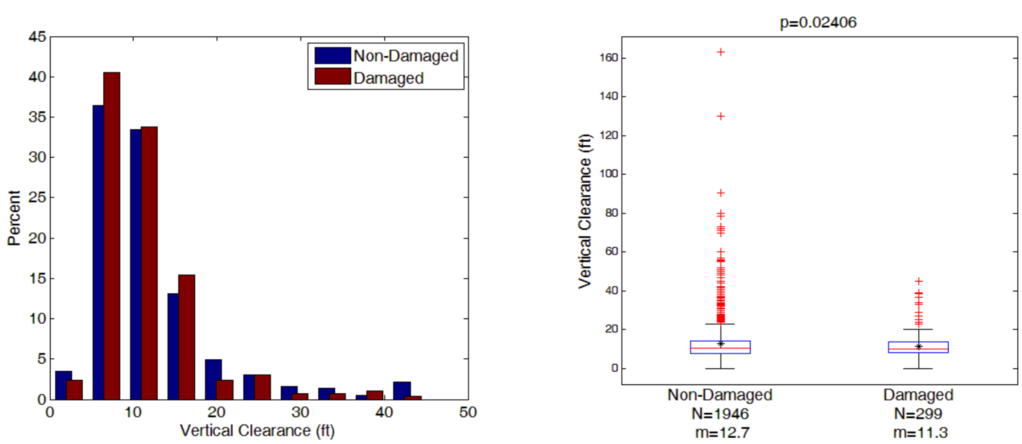

(d) Comparison with respect to the vertical clearance

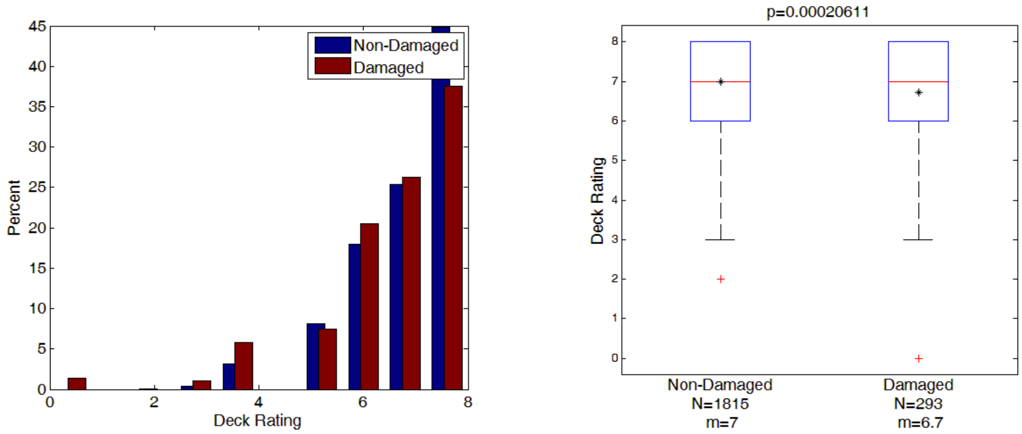

(e) Comparison with respect to the deck rating

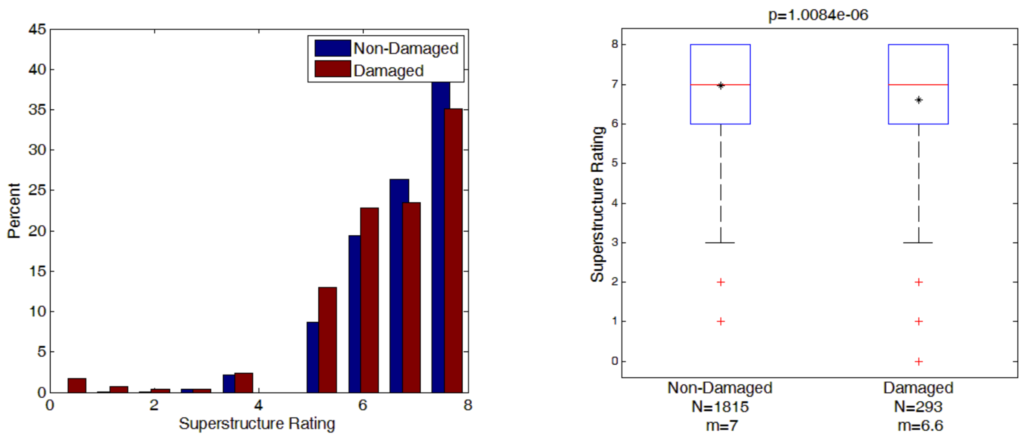

(f) Comparison with respect to the superstructure rating

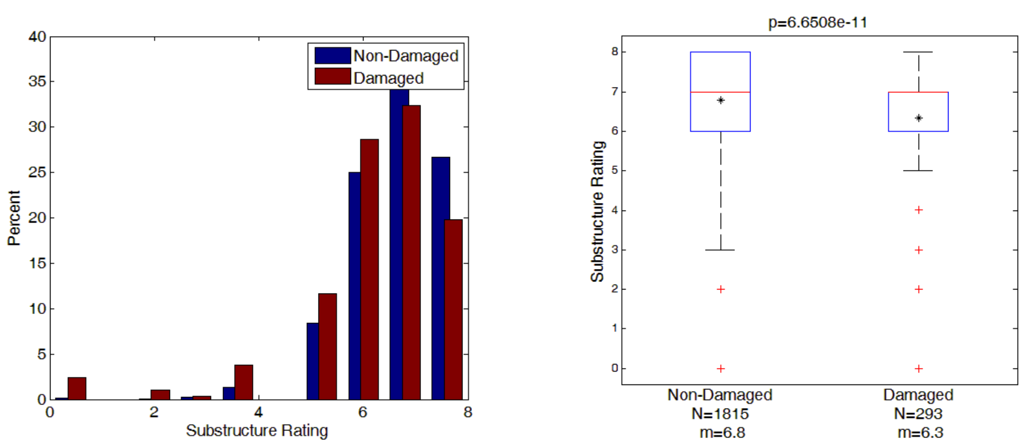

(g) Comparison with respect to the substructure rating

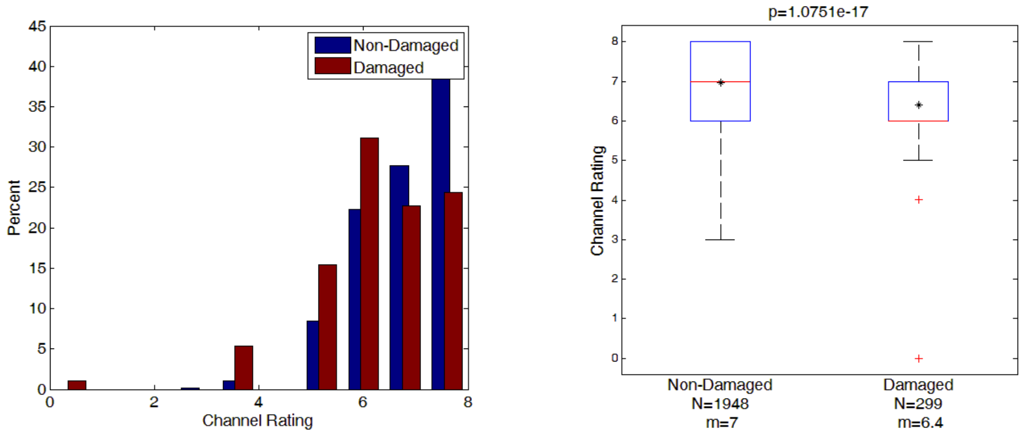

(h) Comparison with respect to the channel rating

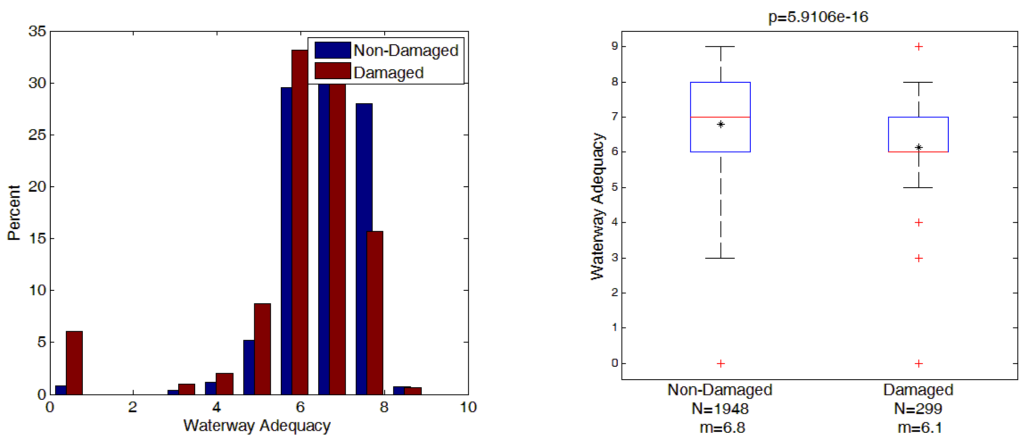

(i) Comparison with respect to the waterway adequacy rating

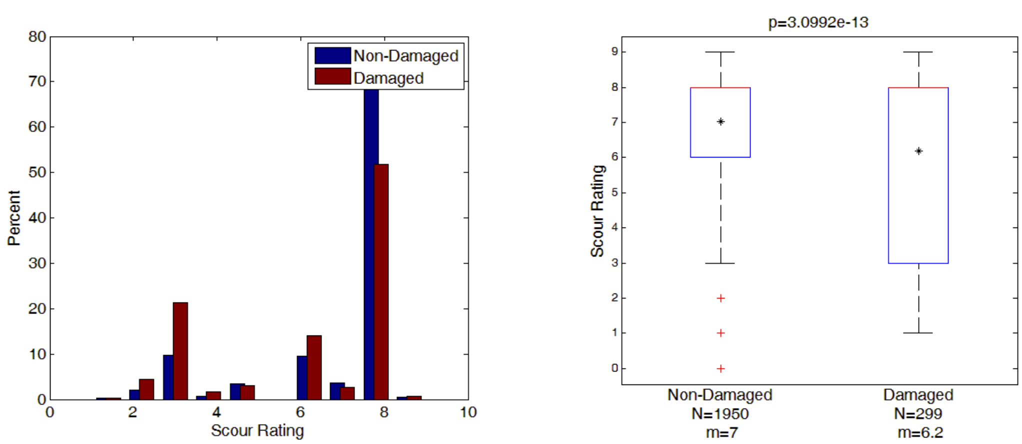

(j) Comparison with respect to the scour rating

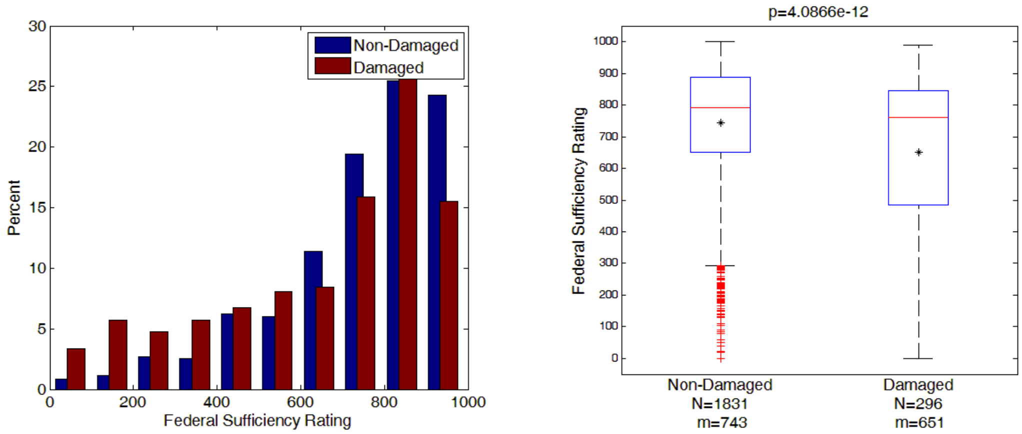

(k) Comparison with respect to the federal sufficiency rating

Figure 2.12: Statistical comparsion of damaged and non-damaged bridges using bridge inspection data

2.7. CONCLUSIONS

The collection of bridge damage information and geospatial joining of it with the available bridge inspection provided a great opportunity for an in-depth look at the characteristics of scour related bridge damage from Tropical Storm Irene. The analysis helps to determine which variables may be worthy of further investigation, and allows for the scope to be narrowed for further study. The geometry variables for bridges did not show a statistical difference between damaged and non-damaged bridges. Bridge ratings showed statistical significance between damaged and undamaged bridges in Tropical Storm Irene indicating that these ratings may be used as a system-level screening tool to identify bridges vulnerable to scour-related damage in extreme events. Although definitive system-level answers as to why certain bridges were damaged in Tropical Storm Irene are still to be determined, it is anticipated that linkages to damage can be made from further analysis of the stream geomorphic conditions from before the storm.

CHAPTER 3

DEVELOPMENT OF A SCOUR SENSOR

3.1. INTRODUCTION

Due to potential severity of scour related damage to bridges, a monitoring system is desired to assess and record the progression of scour and redeposition. Ideally, a scour sensor (or a collection of scour sensors) will measure the evolution (depth and extent as a function of time) of erosion and redeposition, be robust enough to withstand the stream environment, be easy to install at a new or existing bridge, be inexpensive, require minimal energy, be activated as needed, and communicate the measurements to necessary personnel remotely, preferably with a built-in alert system. With these performance requirements in mind, a preliminary design of a new scour sensor (called "Smart Rod") was developed, which is described in this chapter.

3.2. A BRIEF REVIEW OF SCOUR SENSING TECHNOLOGIES

A number of scour sensing technologies have been developed (e.g., scour rod, float out devices, sonar) or currently under development (e.g., time domain reflectometry, smart rocks). Some of these technologies are briefly reviewed below.

3.2.1. Scour Rod

Scour is often measured by personnel on site with a scour rod, which measures the depth of a scour hole at a given point. It can be considered a rigid tape measure. This measurement system is labor intensive, surveyors enter the stream, and manually measure the scour holes. The involvement of human travel and labor makes this process costly and inefficient. Another shortcoming of this scour measuring method is that it does not provide real-time monitoring of scour during high flow events. These instruments are not rugged enough to be used during high flow events and it is dangerous for an individual to go into the field during these events to make measurements (Yu and Yu, 2010). As a result, other methods of scour measurement are preferred.

3.2.2. Float Out Devices

"Float out" means that when the embedded sensor is uncovered by removal of the overlying material, the device will rise to the water surface and act as an early warning system to indicate that scour has occurred on site. There are two types of these devices in use. One of them has the float out portion remaining attached to an object fixed into the riverbed. These systems are reliable but they require a person to go out to the site and observe if the sensor has been deployed. Since an individual still needs to visually check these sensors, there is travel time involved, which often makes this method expensive and inefficient.

Other float out devices travel down river with the current once exhumed from the sediment. This method is simple and removes the need to physically travel to the site. The data are recorded when the device travels downstream. This is accomplished by a detector located at a specific location downstream. This makes the float out device a less feasible option. The early warning device could be lost during its journey downstream. Both variations require the device to be buried in the riverbed. This is an expensive and difficult process due to the amount of physical work and regulations for working in streambeds. Furthermore, excavating soil near a bridge pier may cause problems with the stability of the bridge foundation in the future, and has a one-time use limitation (Hunt, 2012).

3.2.3. Falling collar

Magnetic sliding collars are sensors which use a falling collar to measure the maximum scour depth. As the flow creates a scour hole, the collar falls, registering its position on the rod, allowing for a measurement of the scour depth. Rods can be imbedded in the river bed, or attached to the bridge foundation. The sensor functions with a number of magnetic switches placed at various depths, which activate as the collar passes, are registered in a data logger, and determine the depth. A shortcoming of this technique is that while it will determine maximum scour depth, it will not accommodate the detection of redeposition.

3.2.4. Ultrasonic Method

Alternatively the ultrasonic method uses a Sonic Fathometer and can be described as a sonar method for monitoring scour (Yu and Yu 2010). These devices, much like sonar, send out an ultrasonic pulse to "view" the riverbed. These pulses hit a solid surface and reflect back to the recording device. The further away that object is, the longer the signal takes to get back to the recording device. This system has been used to successfully measure scour in the United States and is currently attached to an estimated 48 bridges (Fisher et al. 2013). This system has proven to be reliable and can measure the development of a scour hole from 0.28 to 1.2 meters in depth (Fisher et al. 2013). Sonar sensors can also be created to withstand hurricane force winds. One of the downfalls of this system is that it is not capable of accurately measuring scour during high turbulence events. This is a concern because turbulence is a characteristic feature of many of the high energy flows that lead to scour. Turbulent waters disturb the ultrasonic pulse, and prevent reliable measures of the riverbed depth. Other problems can be caused when a large amount of air bubbles are present in the water. Figure 3.1 shows how the sensor can also miss the scour hole if the device is not deployed at the correct height. If the device is placed too low then it will not be able to accurately measure the diameter or width of the scour hole. The presence of air bubbles has been known to cause up to 15 ft fluctuations in the data. Another problem with this system is that it cannot accurately take measurements when there is debris in the water. The sonar device will not be able to accurately measure the distance to the riverbed because the ultrasonic pulse will be reflected back to the system once it hits any debris. This causes the riverbed to appear to rise and lower suddenly over short periods of time (Fisher et al. 2013).

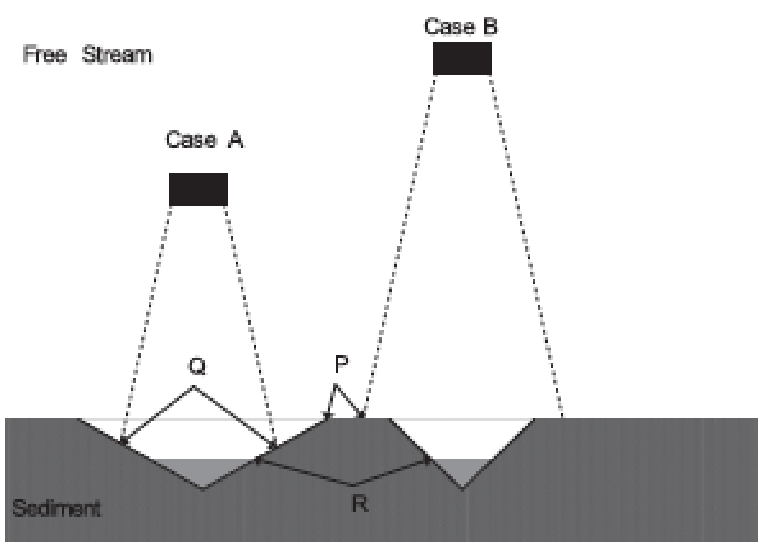

Figure 3.1: Example of one of the limitations of the ultrasonic sensing methods (Fisher et al, 2013)

3.2.5. Time Domain Reflectometry

Scour can also be monitored using a technique called time domain reflectometry (TDR) (e.g. Yu et al. 2013). TDR uses electromagnetic waves to determine the location of the sediment layer. TDR is a common measurement technique for locating damage to power and telecommunications cables, and has appeared in some geotechnical applications, but remains relatively unproven as a scour monitoring technique. The technique uses metal rods to act as waveguides for electromagnetic pulses. The wave speed depends on the dielectric properties of the surrounding medium. This allows the device to measure the interaction between the water and soil. This technology has been found to be more robust and more accurate than sonar devices. Testing has been performed on the accuracy of the TDR under varying conditions, including the salinity of water. An increase in the salinity of the water created a decrease in measurement accuracy. The salt in the water will cause the electromagnetic waves to move more slowly. Slowing of the waves allows a greater chance for the wave to encounter interference, leading to an increased chance of error. Temperature has a similar effect on the electromagnetic wave of the TDR and can render the device inaccurate over varying temperatures (Fisher et al. 2013).

3.2.6. Thermometry

Thermometry sensors are another type of scour sensor that uses a rod as a measurement device. Thermometry devices are often placed in locations with little change in temperature and over long distances, such as the ocean floor along pipelines (Zhao et al. 2012). The thermometry measurement device can be placed into the riverbed or ocean bed horizontally or vertically. The device is designed to measure temperature at different segments of the rod. The sensor can be used to infer scour as follows. There is a difference in temperature or conduction properties between soil and water. When the recorded temperature differs from the norm, assuming the sensor device was initially in soil, it would mean that scour has occurred at that location. Some benefits of the thermometry device are that it is a simple concept to understand and the device has no moving parts that may be lost during high flows. The shortcoming of this type of device is that temperature-reading devices may not be accurate enough to read temperature changes over small intervals. Another problem with the device is that it takes time to set up base data before it can sense a difference between water and soil temperatures. Measuring scour in real time can also be difficult.

3.2.7. Smart Rock

Another experimental scour sensor is known as the Smart Rock. This device has a similar shape and physical properties of a typical piece of rock. The smart rocks are placed into a riverbed at varying elevations. Placing smart rocks into riverbeds often requires some excavation. This initial excavation is a labor-intensive process and may compromise the stability of the bridge. The Smart Rock makes measurements with the use of magnets, which track its rotation in all three axes of movement. This allows the device to measure how the riverbed below moves and changes in depth. Under high flows, it is possible to have forces high enough to cause the rock to move and this movement can also be measured. This technology is still in the experimental stages, and may not work in granular soils. The smart rock may also be incapable of measuring scour during low flow events due to the lack of forces necessary to rotate or move the smart rock. Finally, if the smart rock is washed too far downstream then it may not be recoverable, increasing long-term costs. Each smart rock is a rechargeable unit, which affects long term durability (Chen, 2012).

3.2.8. Fiber Optic Sensors:

Fiber optic sensors have been developed for scour monitoring. Specifically, researchers at the Louisiana Transportation Research Center have used Fiber Bragg Grating sensors to determine bridge scour (Cai et al. 2014). The sensors have the advantage of being corrosion resistant, compact and lightweight, and free from electromagnetic interference. The sensor acts as strain gages, sensing the change in pressure as they are exposed to flowing water. The sensors are arranged on poles, whose bending moment changes as the length of exposed sensor changes, and is used to determine the scour depth. An example of the fiber optic sensor can be seen in Figure 3.2 below. Downsides of the technology include high costs to manufacture, as well as having to rely on complex algorithms to determine the soil water interface.

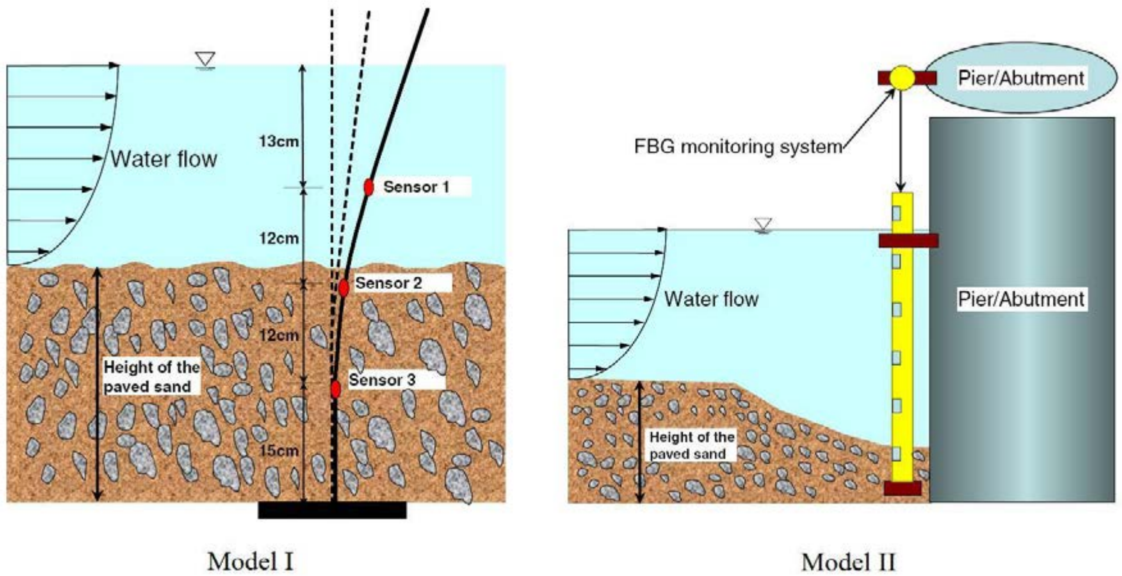

Figure 3.2: Fiber Optic Scour Sensor (Cai et al. 2014)

3.3. PRELIMINARY DEVELOPMENT OF A "SMART ROD" SCOUR SENSOR

3.3.1. Concept

The proposed "Smart Rod" scour sensor consists of acceleration or vibration sensors placed at incremental depths. The sensor arms that extend from the sensor rod remain buried in the bed material until they were exposed by scour. The flow of water activates the sensor, alerting the user of the depth of scour. Recording post scour redeposition is also possible because if deposition occurs, the sensors will cease to move. The sensor device could use segmented components which can be linked together to increase the sensor length to meet site-specific needs. In addition to the motion sensors, temperature sensors could be included to provide a combination of measurements to try to predict the depth of the soil water boundary. A schematic of the sensor concept appears in Figure 3.3. The overall functional scheme of the sensor network is depicted in Figure 3.4.

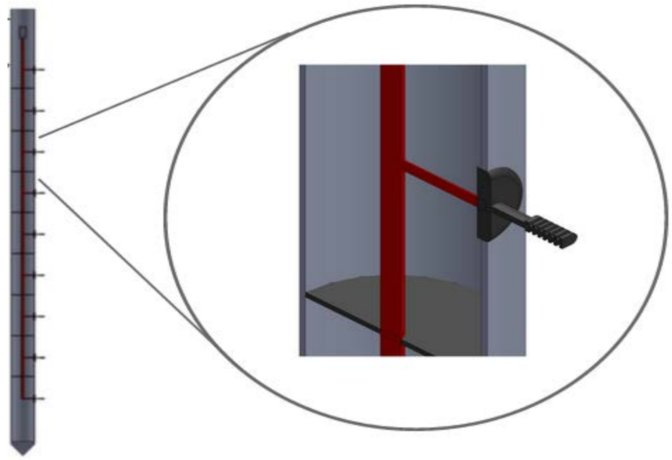

Figure 3.3: Proposed Smart Rod

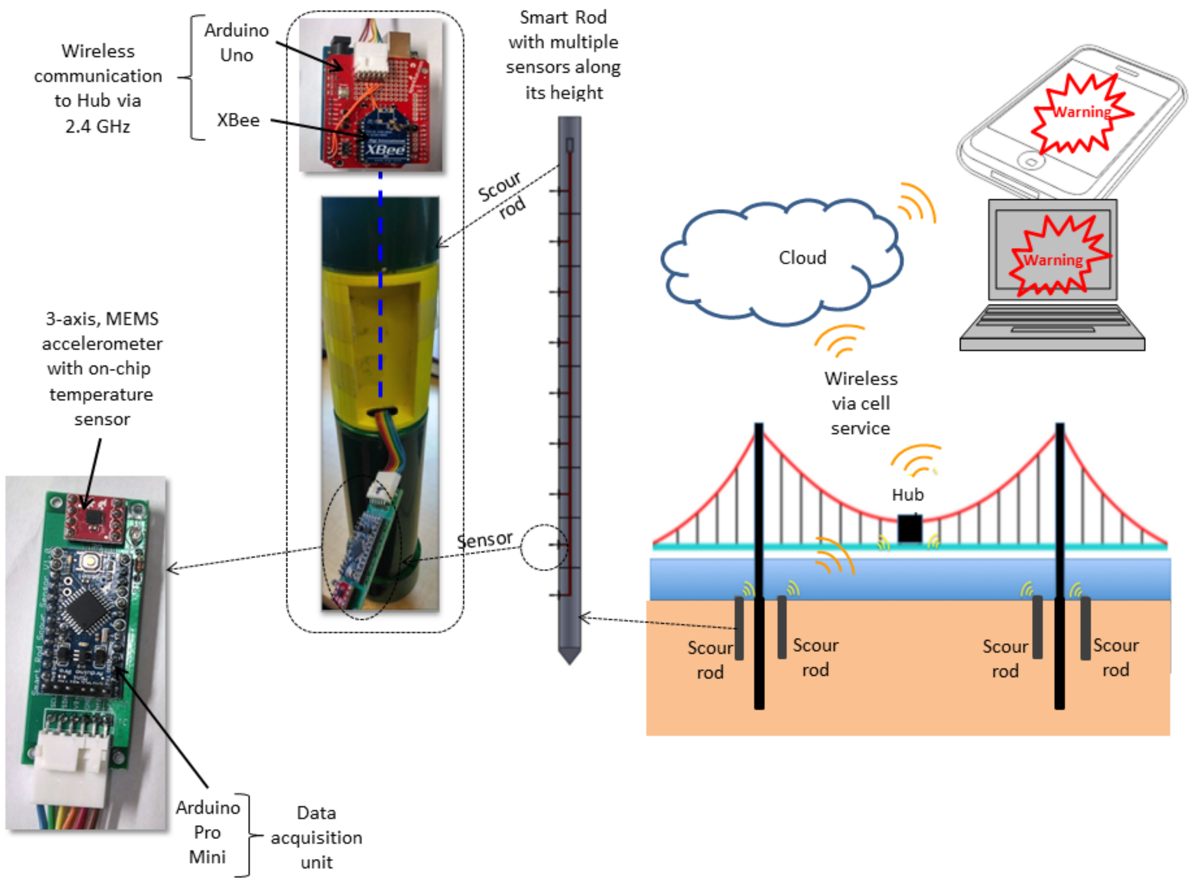

Figure 3.4: Smart Rod scour sensor and communication system

3.3.2. Prototype Sensor Devices

The design of the smart rod can be divided into three main categories: physical, electronic, and programming. The physical components are currently made of PVC pipes and 3D printed components, and in the future that will probably be changed to a non-corrodible metal. Figure 3.5 shows photographs of two prototypes developed thus far. Figure 3.5a shows a unit made out of off-the-shelf PVC pipes and accessories. Figure 3.5b shows a unit developed using components made with a 3D printer.

(a) Using PVC *(b) Using 3D printing*

Figure 3.5: Smart rod prototypes

To describe the electronic components, it is best to start at the sensor and work up through the system. First the movement is sensed by the accelerometer (Sparkfun ADXL362) seen in Figure 3.4. The ADXL362 is a complete 3-axis MEMS acceleration measurement system that operates at very low power consumption levels. Per the manufacturer, it measures both dynamic acceleration, resulting from motion or shock, and static acceleration, such as tilt. The accelerometer is part of an Arduino breakout board. This board has a built in temperature sensor. The reason this particular model was chosen was because it is also programmable. This means that thresholds could be set to determine when the accelerometer alerts the rest of the system.

After the accelerometers gather the data it is interpreted by the next link in the electronic chain, the Arduino Pro Mini, also seen in Figure 3.6. This device interprets the serial data coming from the accelerometer and then converts it into a more suitable format, including the addition of sensor location and timing information to digital data.

The next step is to transmit the data, from the Arduino Pro Mini to the Arduino Uno. The Arduino Uno is the cap board, seen in Figure 3.7. This interprets the data from the various Pro Mini and accelerometer combinations to determine if any of the sensors are activated. The benefit of having the Pro Minis sending out digital data is that there only has to be one set of wires running down the entire length of the sensor array. The Arduino Uno will determine if any of the sensors are activated, and if they are, it will transmit data wirelessly to the data logging hub.

Attached to the Arduino Uno is the Xbee, as seen in Figure 3.7. This is a wireless communication unit that can easily be networked with other Xbee's operating on the same frequency. These devices allow for two way communication which allows the users to get the data if they want to check on the sensors outside of the normal communication schedule. The Xbee sends the data to the data logging hub.

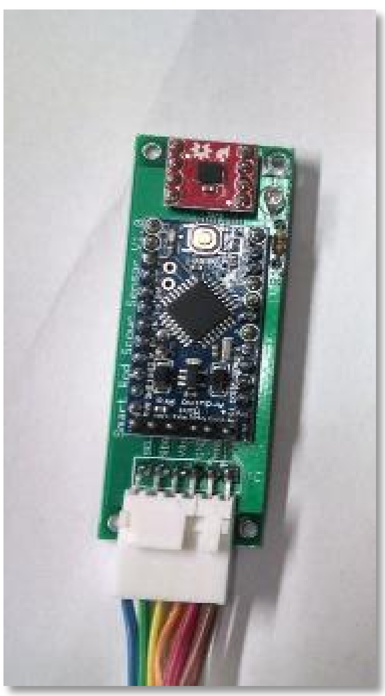

Figure 3.6: Accelerometer (red) and Arduino Pro Mini (blue)

Figure 3.7: Arduino Uno (red) and Xbee (blue)

The central data logger and communication hub uses either a renewable power source or can be wired into the normal power grid. The purpose of this part of the system is to transmit the data gathered from the sensors to the stake holders who will be located off-site. This will be accomplished with a 900MHz Xbee. This device is connected to power, and as a result, it will be able to sustain the longer range communications.

3.3.3. Programming

Back End, Arduino:

The back end programming controls how the sensors will react in various operational situations. Through the back-end programming, thresholds can be set and the temperature data can be recorded. If there are any changes in either of the two measurements then the stakeholders can be alerted.

Currently the code can be broken into two major categories. The first is the code on the Arduino Pro Mini. This code controls how the sensors are calibrated for temperature and acceleration. This code also determines the sampling frequency of the accelerometers. The code on the Arduino Pro Mini give the data coming from a specific accelerometer a unique sensor ID so that the cap Arduino knows which of the sensors it is receiving data from. This works because the Arduino Pro Mini pulls an interrupt pin that will wake the Cap Arduino Uno out of a sleep mode. At this point it is the task of the Arduino Uno located at the Cap of the rod to determine which sensor is active. Thresholds can be set within the Arduino Pro Mini to manage when it alerts the Cap Arduino. This allows the device to alert the cap if there is a large deviation from the normal safe state. The ID can be programed to allow for modularity of the sensors on a single smart rod.

The sensors are smart enough to ensure that they do not all try to send data at the same time. To prevent this, they are programmed check to see if the interrupt has been activated already. If it has been activated then they delay sending data for one sensing cycle. This basically ensures that they will organize themselves in such a way that they do not ever try to send data at the same time. Ordinarily this would not be a problem but due to the fact that these sensors only have one line of communication to share it becomes important. The reason there is only one line of wire is to allow the system to be modular.

The Cap Arduino or the Arduino Uno is the brains of the operation. It determines which one of the sensors are active on a single rod. Then it pairs this information with a unique rod identifier. This rod identifier is another number that will tell the user which rod has been activated in situations where multiple smart rods are used at a given site. Through the use of these two identifiers, the depth and extent of scour can potentially be pinpointed. This code is also responsible for sending the data wirelessly. To ensure that the wireless communication units do not try to send data at the same time, they check in and see if one of the other sensors is sending anything. If one of the other sensors is sending data at that time then they wait for tenth of a second and check again. When the other rod is not sending data, then data can be sent without any conflict.

Front End Interface:

A control center interface, currently in MATLAB, was developed to help interpret the data transmitted from an array of Smart Rods in a user-friendly and remotely accessible arena. The idea was to develop a visual display desktop shortcut to allow a user to easily monitor a site in real-time while also maintaining the functionality to index into logged data from the past. The display acts as an early warning system notification center to interpret dangerous levels of scour and erosion from uniquely identified sensors to indicate the exact location of the concerning scour development. The software also enables system calibration parameters to be altered by the user while (continuously) indexing time-stamped data transmitted wirelessly from the site. The user can alter thresholds that trip the warning message display. Built-in and specifically designed MATLAB functions were used for the serial data import as well as the graphical window and alarm message displays.

The software catalogues data transmitted from the Xbee antenna, documenting smart rod number, sensor number, acceleration in the z-axis, and temperature in degree centigrade. The data are assigned to a variable specified within the program. A function within the software program was designed to save the contents of the data at a desired time interval. The contents of the data variable are saved as a plain text file and time-stamped to encourage easier indexing. If the change in acceleration surpasses a set threshold, an alarm message will be displayed indicating the sensor number (location) and smart rod number (location). The program is able to draw conclusions based on the threshold. The change in acceleration indicates that the sensor was unearthed, or scour has developed at that location. The smart rod and sensor numbering system were designed to interact with a site-specific smart rod array, helping to indicate where the scour has developed and to what extent.

Testing is being continued to further determine the practicality of using temperature as a surrogate measure for scour. Additionally, more interface analytics could be developed to create a river and stream bed elevation profile. This could be based on initial depths at which the smart rod array was installed on site as well as the changes that occur over time due to scour and redeposition.

3.3.4. Testing Results

Many experiments were conducted to assess the functionality of the Smart Rod prototype, and also determine areas that need to be developed further. The following section is a summary of the results attained during the testing process. Three different experiments were used to analyze the prototype (i.e. wireless communication capability, accelerometer functionality, and temperature sensor functionality).

Communication between the sensor rod and the data logger needs to be reliable and informative. In order to have an understanding of the wireless capability of the device, the sensor rod was placed at multiple locations, and capable of recording reliably up to 37 feet, through multiple objects and floors of a building. This is a smaller distance than the 300 feet an Xbee manufacturer reports. However, this is the expected result since testing was done inside of a building with many obstacles. The testing location had more signal suppressing objects, which would most likely be fewer in a natural setting. The device signal is considered to be reliable up to 40 feet, in an area of numerous signal suppressing objects. Accelerometers were the chosen sensor type for the Smart Rod to quantify the depth of scour in a streambed. Many tests focused on determining the accuracy and ability of the prototype sensor to record scour and deposition. There were two different tests that were performed to analyze the accelerometers (i.e. 5-gallon bucket tests and flume tests). The results of these tests show that the accelerometers are very useful and reliable in determining the occurrence of scour. The sensors displayed a change in reading when they were uncovered by scour. The device does not record as originally thought; they "sense" position rather than acceleration. This change in position can still be used to determine when the sensor becomes exposed. Testing showed that accelerometers have a steady reading when buried within the soil, but start to "flutter" once they are exposed. The average "flutter" (i.e. the difference between maximum and minimum readings within a five second interval) that the device saw was around 0.08g (Table 3.1). This number is smaller than what was expected, but is still easily recognizable. The result of the small flutter is due to many factors, one being that the current sensor connection to the sensor rod is very stiff. This prevents the sensor from bending significantly. In the future, different connections will need to be experimented with so the sensor has a larger range of movement.

To assess the best orientation for the sensor installment, the sensor was placed, fully exposed, at different angles to flow (i.e. parallel to flow and at a 45^{o} angle). The best orientation to place the sensor was directly behind the sensor rod (i.e. the sensor downstream of the sensor rod and parallel to flow). This makes sense, as this is a point of high turbulence, the flow of water is “merging” back together after traveling around the sensor rod. When a sensor rod is placed at an angle the flutter decreases significantly. This could be a result of the water velocity being stable while traveling around the rod and becoming turbulent as the flow separates downstream of the rod. The difference in readings could also be a result of the prototype currently recording only one axis of movement, rather than all three axes.

<u>Temperature Sensor:</u>

The accelerometers used for the smart rod prototype have a built-in temperature sensor. The relationship between sensor output and actual temperature is linear, as seen in Figure 3.8. It is to be noted that the sensor unit was coated with insulation. The effect of insulation (type and extent) on the sensor calibration is not yet investigated.

Table 3.1: The Accelerometer Results of Flume Testing

Setup	Depth to Sensor	Flume Flow Rate	Trigger	Time	Flutter	Notes
-	cm	hertz	y/n	min	0.01g	-
Flume setup with scour aid						
	7.5	10.5- 12	yes	11	0.01	The flow of water was gradually increased from 10.5 to 12 because scour was too slow at low flow
	0	12	yes	0	0.04	
	4	12	yes	1	0.05	
Flume setup without scour aid and sensor installed parallel to flow						
	5	20.00	no	60	0	The device did not seem to flutter much, however there was a noticible difference in flutters when the wire became exposed. The device seemed to also become impacted by the hydraulic jump that occurred due to the front weir.Flow gradually increased due to scour development being slow.
	0	20	yes	0	0.08	The device was placed fully exposed in the river bed.
Flume setup without scour aid and sensor installed at a 45^{o} angle to flow						
	4	23	no	40	0	Scour was not occuring around the sensor rod and so testing was stopped.
	0	23	yes	0	0.03	Sensor was placed fully exposed into riverbed

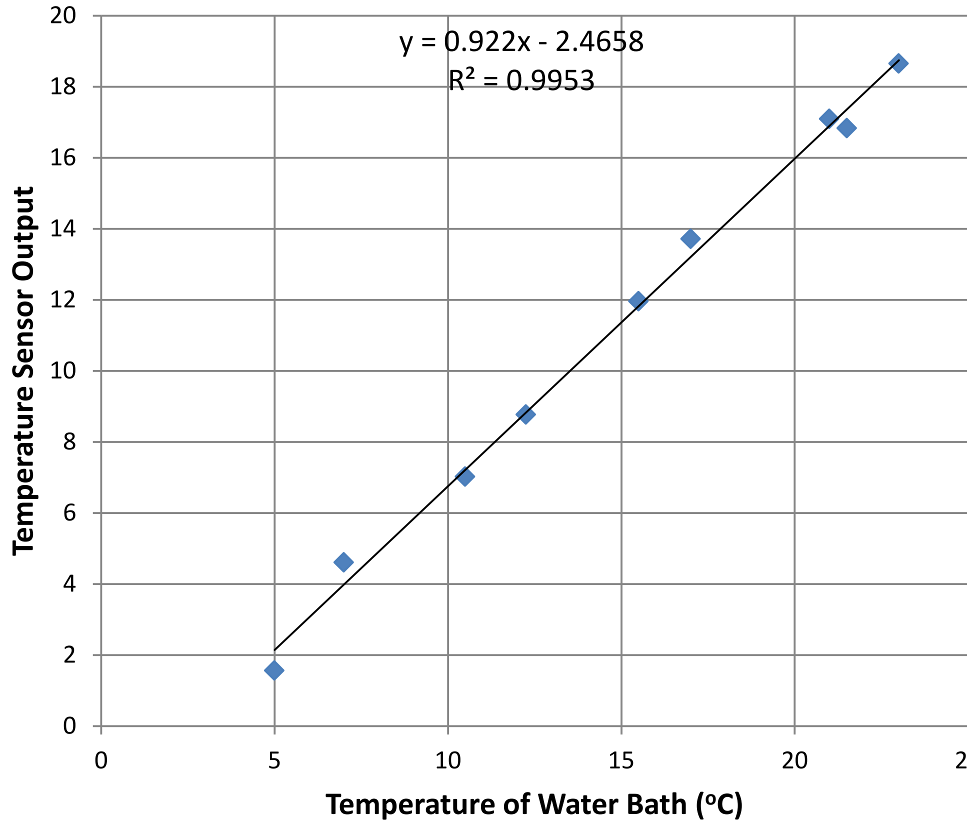

Figure 3.8: Temperature sensor output vs. the temperature

An experiment set up to mimic a groundwater fed stream was setup in a 6 m x 1 m recirculating flume (Figure 3.9). The test had two distinct temperature profiles, a warm stream flow, and cold groundwater. An ice-bath was used to produce the cold groundwater supply. Once the sensor had reached equilibrium with the groundwater supply, a scour aid was set up to erode the soil above the sensor. Figure 3.10 shows the resulting temperature over time, using the temperature sensor on the rod. The sensor response was consistent over the first portion of the test while the temperature was changing slowly. However during the second portion of the test the accuracy of the temperature reading is less reliable due to the increased rate of temperature change. As scour occurs above the sensor, the sensor records a higher temperature (the flume water is warmer than the water within the soil). The rise in Figure 3.10 at the 20-minute mark is due to an increase in the flume velocity. The increase in velocity increases the rate of scour, which can be seen as greater recorded temperature change during this time. The temperature sensor was capable of picking up both rapid scour production and degradation scour.

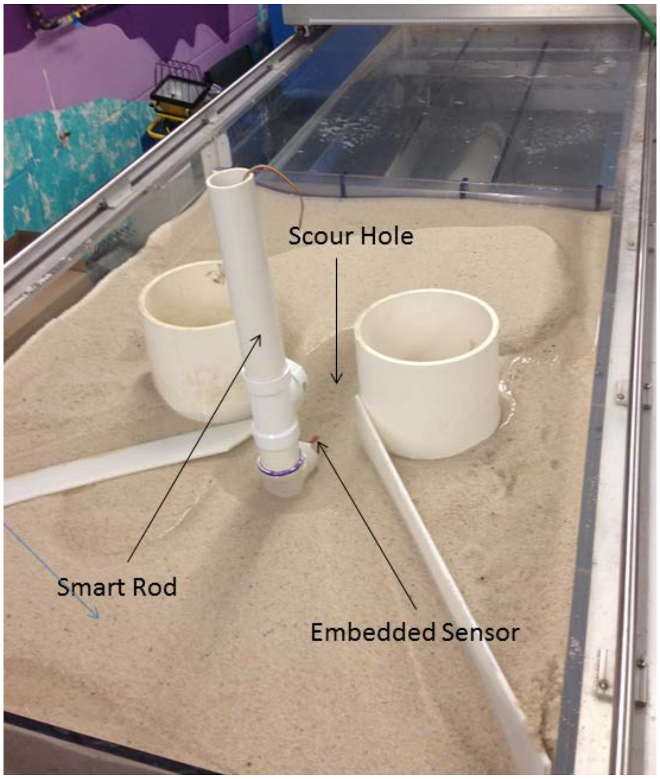

Figure 3.9: Experimental set-up to intentionally generate scour in a recirculating flume

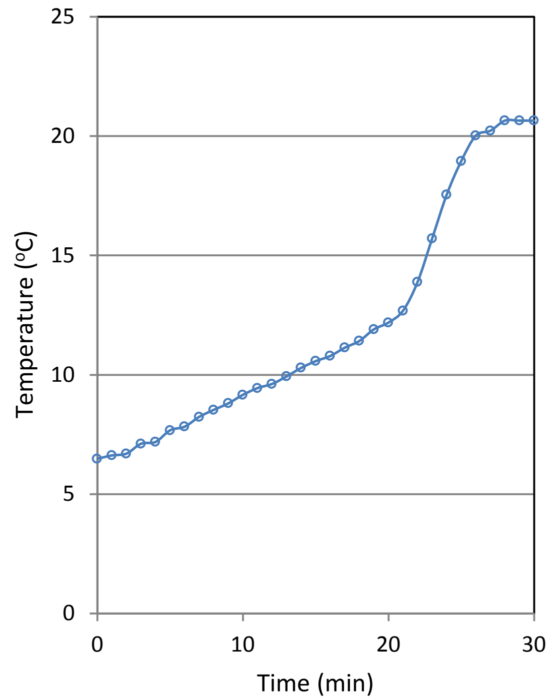

Figure 3.10: Temperature vs. Time Using a Scour Aid and a Cold Groundwater Supply

The temperature sensor readings change when placed within different temperature water, so they can potentially be used to determine scour and erosion in a riverbed. In order to increase the reliability of the temperature sensors, a sensor should be placed above the riverbed. This could then be used as a base to indicate the difference between flowing water and groundwater.

3.4. CONCLUSIONS

The following conclusions are drawn for this component of the research:

1) The proposed Smart Rod scour sensor has the potential to be low-cost and ability to overcome many of the shortcomings of other types of scour sensors.

2) Early stage prototype development and testing of the sensor indicated the potential viability of the Smart Rod concept.

3) The follow up work will have to include development of a robust physical design of the Smart Rod so it can be deployed in the field environment. Efficient field installation methods would

also have to be developed. Field deployment of a number of Smart Rods and assessment of their performance under a variety of operational scenarios (existing versus new bridges, high flows, different river bed types, different seasons, etc.) would also be necessary.

CHAPTER 4

FUTURE WORK

Future work to assist in the prediction and mitigation of the effects of scour on Vermont Bridges include the continued development of the Smart Rod scour sensor, and the continuation of the evaluation of bridge database.

The Smart Rod scour sensor will go through another round of development and prototyping. The concept of acceleration, vibration, and/or temperature detection for scour prediction has been tested successfully. Further development is needed for a robust deployment of these technologies. The Smart Rod scour sensor using motion and temperature sensing could provide an inexpensive and robust scour prediction, with the ability to report scour and deposition real time wirelessly integrated into a warning system.

As a continuation of the bridge inspection database analysis, stream geomorphic data available from the Vermont Agency of Natural Resources' Rapid Geomorphic Assessment will be utilized. The addition of stream geomorphic data will allow for stream geometry and stability metrics to aid in the assessment of potential for bridge scour. The large amount of data available through bridge inspection and stream geomorphic data will allow for an in-depth analysis on the bridge health, stream stability, and bridge-stream interactions. Additionally, multiple scales, from statewide, to a reach based analysis can be conducted to determine the range at which the available data is geospatially statistically significant.

REFERENCES

Arneson, L. A., Zevenbergen, L. W., Lagasse, P. F., and Clopper, P. E. (2012). Evaluating Scour at Bridges. Fifth Edition, Hydraulic Engineering Circular No. 18, Federal Highway Administration, Washington, D.C.

Betts, A. (June 2011, edited 10/29/2011). Climate Change in Vermont. Available at: http://www.anr.state.vt.us/anr/climatechange/Pubs/VTCCAdaptClimateChangeVTBetts.pdf. Accessed: 17 November 2011.

Chen, G., Pommerenke, D., and Zheng. R. Y. (2012) “Smart Rocks and Wireless Communication Systems for Real- Time Monitoring and Mitigation of Bridge Scour.” Missouri University of Science and Technology (April 19, 2012).

Cai C.S., Kong X., Xiong W., Hou S., (2014) “Monitoring Bridge Scour Using Fiber Optic Sensors.” Louisiana Transportation Research Center. FHWA/LA.10/535

Federal Highway Administration. (2015), Recording and Coding Guide for the Structure Inventory and Appraisal of the Nation's Bridges. Report No. FHWA-PD-96-01, U.S. Department of Transportation, Washington, D.C.

Fisher, M., Chowdhury, N., Khan, A., Atamturktur, S., (2013). “An Evaluation of Scour Measurement Devices.” Flow Measurement and Instrumentation 33, no. 0 (2013): 55 – 67. http://dx.doi.org/10.1016/j.flowmeasinst.2013.05.001.

Frumhoff, P.C., J.J. McCarthy, J.M. Melilo, S.C. Moster, and D.J. Wuebbles (2007). Confronting Climate Change in the U.S. Northeast: Science, Impacts, and Solutions. Synthesis report of the Northeast Climate Impacts Assessment Team (NECIA), Union of Concerned Scientists. Available at: http://www.climatechoices.org/ne/resources_ne/nereport.html. Accessed 17 November 2011.

Gee, K.W. (2008). Action: Technical Guidance for Bridges over Waterways with Unknown Foundations, Federal Highway Administration, Washington, D.C., http://www.fhwa.dot.gov/engineering/hydraulics/policymemo/20080109.cfm. Accessed June 2014

Hunt, B. E., Shields G. M., and Price, G. (2012). “New Directions in Scour Monitoring.” AECOM, August 27, 2012. http://vzb.baw.de/publikationen.php?file=icse6/0/7_249_ICSE-6_Hunt_Scour_Monitoring_For_Posting-vreduite.pdf.

Hunt, B. E. (2009). Monitoring Scour Critical Bridges (Vol. 396). Transportation Research Board.

Kattell J, Eriksson M (1998) Bridge Scour Evaluation: Screening, Analysis, and Countermeasures. USDA Forest Service, No. 9877: San Dimas Technology and Development Center.

Lagasse, P. F., Zevenbergen, L. W., Schall, J. D., & Cloper, P. E. (2009). Bridge scour and Stream Stability Countermeasures: Experience, Selection, and Design Guidance-Third Edition. Hydraulic Engineering Circular 23 (HEC-23). Report FHWA-NH1-01-003. Federal Highway Administration, Washington, DC.

Melillo, Jerry M., Terese (T.C.) Richmond, and Gary W. Yohe, Eds. (2014) Climate Change Impacts in the United States: The Third National Climate Assessment. U.S. Global Change Research Program, 841 pp. Doi: 10.7930/J0Z31WJ2.

National Weather Service. (2011). Preliminary Hurricane/Tropical Storm Irene Weather Summary for the North Country. National Weather Service Forecast Office, Burlington VT, http://www.erh.noaa.gov/btv/events/Irene2011/. Accessed July 2014

Stager, J.C. and M. Thill. (2010). Climate Change in the Champlain Basin: What natural resource managers can expect and do. Available at: http://www.nature.org/ourinitiatives/regions/northamerica/unitedstates/vermont/howwework/champlain_climate_report_5_2010.pdf. Accessed: 11 November 2011.

Thomas, P., Jones, T., Azizi, S.C., (2013). Jousting with Bridges. FEMA’s Historic Preservation Section, Joint Field Office, Essex Junction, VT

U.S. Geological Survey, (2011). High flows in New Hampshire and Vermont from tropical storm Irene estimated. U.S. Geological

Survey,http://nh.water.usgs.gov/whatsnew/Irene_aug2011.htm. Accessed July 15, 2014

Vermont Agency of Transpiration (2014). Engineering Image Archives. State of Vemont Agency of Transposition Office, Montpeiler VT, http://vtransmap01.aot.state.vt.us/rp/dpr/Diphotowebstore//dpr.asp Accessed June 2014

Yu, X., and Yu X. (2010). "Laboratory Evaluation of Time-Domain Reflectometry for Bridge Scour Measurement: Comparison with the Ultrasonic Method." Advances in Civil Engineering 2010 (2010): 1-13. Hindawi. Hindawi Publishing Corporation, 2010.

Yu, X., Zhang, B., Tiao, J., and Yu, X. (2013), “A new time-domain reflectometry bridge scour sensor”, Structural Health Monitoring, 12(2), 99-113.

Zhao, X., Li, L., Ba, Q., and Ou, J., (2012) “Scour Monitoring System of Subsea Pipeline Using Distributed Brillouin Optical Sensors Based on Active Thermometry.” Optics & Laser Technology 44, no. 7 (2012): 2125 – 2129. doi:http://dx.doi.org/10.1016/j.optlastec.2012.03.015.